

Generalized dynamical density functional theory for classical fluids and the significance of inertia and hydrodynamic interactions

Benjamin D. Goddard¹, Andreas Nold^{1,2}, Nikos Savva¹,
Grigorios A. Pavliotis^{3,4}, and Serafim Kalliadasis¹

February 16, 2012

Abstract

We study the dynamics of a colloidal fluid in the full position-momentum phase space. The full underlying model consists of the Langevin equations including hydrodynamic interactions, which strongly influence the non-equilibrium properties of the system. For large systems, the number of degrees of freedom prohibit a direct solution of the Langevin equations and a reduced model is necessary, e.g. a projection of the dynamics to those of the reduced one-body distribution. We derive a generalized dynamical density functional theory (DDFT), the computational complexity of which is independent of the number of particles. We demonstrate that, in suitable limits, we recover existing DDFTs, which neglect either inertia, or hydrodynamic interactions, or both. In particular, in the overdamped limit we obtain a DDFT describing only the position distribution, and with a novel definition of the diffusion tensor. Furthermore, near equilibrium, our DDFT reduces to a Navier-Stokes-like equation but with additional non-local terms. We also demonstrate the very good agreement between the new DDFT and full stochastic calculations, as well as the large qualitative effects of inertia and hydrodynamic interactions.

1 Introduction

Since the experimental discovery of the Brownian motion of pollen particles in water in the 19th Century[1], the study of classical fluids (systems of particles at sufficiently high temperature so that quantum effects can be neglected), such as colloidal systems, has been fundamental not only to the development of statistical mechanics starting from the work of Einstein[2], Langevin[3] and Smoluchowski[4], but also to many other fields in physics, chemistry and engineering, e.g. the evolution of microscopy over the last century[5, 6, 7], recent advances in biophysical research[8] and the rapidly-growing field of microfluidics[9, 10, 11]. Colloidal systems, in particular, are versatile model ones for both theoretical and experimental scrutiny, e.g. many of the forces governing their structure and behaviour govern also the structure and behaviour of matter, whilst the sufficiently large physical size of colloidal particles makes them accessible experimentally. The large number of particles present in real-world systems translates to high-dimensional mathematical models which quickly become computationally intractable.

Statistical mechanics approaches, such as dynamical density functional theory (DDFT)[12], allow the dynamics of systems of arbitrarily large numbers of particles to be studied. However, existing DDFTs neglect either the momentum of the colloidal particles[13], or the hydrodynamic interactions mediated through the bath[14], or both[15]. Yet, inertial effects are negligible only

¹ Department of Chemical Engineering, Imperial College London, London, SW7 2AZ, United Kingdom. ² Center of Smart Interfaces, TU Darmstadt, Petersenstr. 32, 64287 Darmstadt, Germany. ³ Department of Mathematics, Imperial College London, London, SW7 2AZ, United Kingdom. ⁴ CERMICS, Ecole Nationale des Ponts et Chaussées, 6 & 8 Avenue Blaise Pascal, 77455 Marne La Vallée Cedex 2, France.

in the high-friction limit[16], whilst hydrodynamic interactions are long range[17]; it is therefore unclear that existing DDFTs are sufficiently accurate to model colloidal systems of general applicability. Here we outline a generalized DDFT formalism which includes hydrodynamic interactions in the full position-momentum phase space description. In particular, we recover existing DDFT formulations[15, 13, 14] as special cases and we further demonstrate the effects and implications of including hydrodynamic interactions and inertia. The new DDFT is validated with stochastic simulations.

The careful inclusion of both inertia and hydrodynamic interactions is a large step towards accurate and predictive modelling of physically-relevant systems. The numerical experiments presented here for model cases of hard spheres in spherically-symmetric external potentials should serve as a solid starting point for a wide range of applications.

2 The Langevin and Fokker-Planck Equations

We are interested in systems consisting of a large number N of identical, spherically symmetric colloidal particles of mass m suspended in a bath of many more, much smaller and much lighter particles. Typically, colloidal particles have sizes ranging from 1nm – $1\mu\text{m}$, occupying the same volume as approximately 10^7 – 10^{10} water molecules. As such, treating the bath particles exactly is computationally prohibitive. However, a typical timescale for a colloidal particle to diffuse a distance equal to its diameter is 1s , whilst the typical time between collisions of water molecules is 10^{-15}s [18]. Hence, if we are interested in timescales significantly larger than this typical collision time, we may introduce a coarse-grained model and consider only the positions and momenta of the colloidal particles, treating the bath in a stochastic or probabilistic manner.

This approximation leads to the Langevin[3] (or stochastic Newton's) equations for the $3N$ -dimensional colloidal position and momentum vectors $\mathbf{r} = (\mathbf{r}_1, \dots, \mathbf{r}_N)$ and $\mathbf{p} = (\mathbf{p}_1, \dots, \mathbf{p}_N)$ with \mathbf{r}_i and \mathbf{p}_i the position and momentum of the i th particle:

$$\frac{d\mathbf{r}}{dt} = \frac{\mathbf{p}}{m}, \quad \frac{d\mathbf{p}}{dt} = -\nabla_{\mathbf{r}}V(\mathbf{r}, t) - \mathbf{\Gamma}(\mathbf{r})\mathbf{p} + \mathbf{A}(\mathbf{r})\mathbf{f}(t). \quad (1)$$

Here, V is the potential, which is generally a sum of an external potential, such as gravity, and inter-particle forces, such as electrostatic effects. The first equation shows that the change in position is given by the velocity, whilst the second shows that the change in momentum is given by the force, the first part of which is the negative of the potential gradient. The final two terms model the effects of the bath. The motion of the colloidal particles causes flows in the bath, which in turn cause forces on the colloidal particles, called hydrodynamic interactions (HI); see Figure 1(a) for an illustrative sketch. The momenta and forces are related by the $3N \times 3N$ positive-definite friction tensor $\mathbf{\Gamma}$, a generalisation of self-friction tensor $\gamma\mathbf{1}$, where $\mathbf{1}$ is the $3N \times 3N$ -dimensional identity matrix and γ is the friction felt by a single isolated particle. Collisions of bath particles with colloidal particles are described by the stochastic forces \mathbf{f} , given by Gaussian white noise. The strength of these collisions is related to $\mathbf{\Gamma}$ via a generalized fluctuation-dissipation theorem[19], giving $\mathbf{A} = (mk_B T \mathbf{\Gamma})^{1/2}$, where T is the temperature and k_B is Boltzmann's constant. Note that here and in the following we have assumed that T is constant in space, i.e. that the solvent bath is also a heat bath, equilibrating on a much faster timescale than the particle dynamics.

Equations (1) are normally solved numerically by a time-stepping algorithm such as the Euler-Maruyama scheme[20]. If HI are neglected by setting $\mathbf{\Gamma} = \gamma\mathbf{1}$ then $\mathbf{A} = (mk_B T \gamma)^{1/2}\mathbf{1}$ is known explicitly and the numerical solution of (1) takes $O(N)$ operations at each timestep. In contrast, including HI requires \mathbf{A} to be determined from $\mathbf{\Gamma}$, e.g. through Cholesky decomposition, which then increases the operations required for the numerical solution to $O(N^3)$. Hence, since N is large, HI are often neglected to reduce the computational cost, whereas physically they are important in all but very dilute systems as they decay only with the inverse of particle separation[17, 21]. Figure 1 demonstrates the effects of including HI in a very simple system, nine identical hard-sphere colloidal particles subject only to a constant vertical force -1 with $\gamma = 1$. If HI are neglected, the particles accelerate vertically until reaching terminal velocity. Including HI not only increases

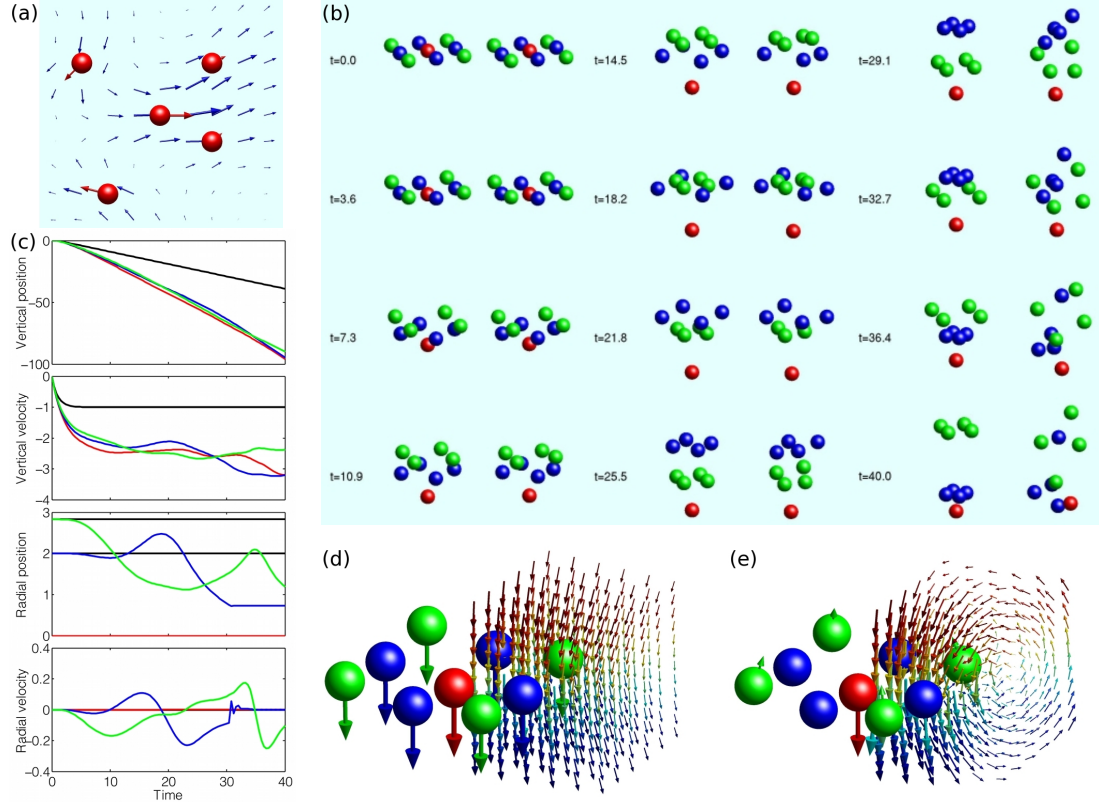


Figure 1: Dynamics of hydrodynamically-interacting particles. (a) Bath fluid flows (*blue*) induced by motion of spherical colloidal particles (*red*) restricted to a plane. (b)–(e): Motion of nine identical hard-sphere colloidal particles, coloured by symmetry, under a constant vertical force and HI at zero temperature (solution of (1)). (b) Evolution in the centre of mass frames with (*left*) completely symmetric square lattice and (*right*) slightly perturbed initial conditions. (c) Vertical and radial (from centre particle in horizontal plane) positions and velocities of corresponding coloured particles for symmetric initial condition. Black curves correspond to no HI. Colloid velocities and bath flows in (d) laboratory reference frame and (e) centre of mass frame. Bath flow coloured by vertical position. Other quadrants are symmetric. See also Supplementary Movie 1.

the speed of sedimentation, but also introduces complex oscillatory dynamics caused by the flows in the bath induced by the particle dynamics, which are circulatory when viewed in the centre of mass frame; see Figure 1(e). Note that both self-interactions and lubrication effects have been neglected. Whilst the former may be measured experimentally[6], they are negligible on the timescales described here. However, neglecting lubrication effects leads to a kink in the radial velocity (at around non-dimensional time 30) due to the hard sphere effects.

When N is large, a particular realization of the dynamics of particles, as given by (1), is irrelevant as it is practically impossible to know the exact initial conditions and, as can also be seen from Figure 1(b), a small perturbation in initial conditions can lead to vastly different long-time dynamics. What is of interest are average quantities over a large number of experiments, or a large number of realizations given by (1). Mathematically, this corresponds to the joint probability distribution $f^{(N)}(\mathbf{r}, \mathbf{p}, t)$, which is the probability of finding the particles with positions \mathbf{r} and momenta \mathbf{p} at time t .

Averaging the Langevin equation (1) over the initial particle distribution and the noise leads to the Kramers equation (the corresponding Fokker-Planck equation in phase space), a $6N$ -dimensional deterministic partial differential equation for the evolution of the distribution function:

$$\begin{aligned} 0 = \partial_t f^{(N)}(\mathbf{r}, \mathbf{p}, t) &+ \frac{1}{m} \mathbf{p} \cdot \nabla_{\mathbf{r}} f^{(N)}(\mathbf{r}, \mathbf{p}, t) \\ &- \nabla_{\mathbf{r}} V(\mathbf{r}, t) \cdot \nabla_{\mathbf{p}} f^{(N)}(\mathbf{r}, \mathbf{p}, t) \\ &- \nabla_{\mathbf{p}} \cdot [\mathbf{\Gamma}(\mathbf{r})(\mathbf{p} + mk_B T \nabla_{\mathbf{p}}) f^{(N)}(\mathbf{r}, \mathbf{p}, t)] \end{aligned} \quad (2)$$

Note that this transformation does not reduce the numerical complexity, as taking M discretization points for each spatial/momentum dimension would require $(2M)^{3N}$ points in total; the only way to solve the Kramers equation in high-dimensions is by using Monte Carlo methods, i.e. by solving (1). However, it is known rigorously[22] that $f^{(N)}$ is a functional of the one-body position distribution $\rho(\mathbf{r}_1, t) = N \int d\mathbf{p} d\mathbf{r}' f^{(N)}(\mathbf{r}, \mathbf{p}, t)$, where $d\mathbf{r}'$ denotes integration over all but \mathbf{r}_1 , the position of the first particle. Hence, for any number of particles at fixed time, the system is, at least in principle, completely described by a function of only a single three-dimensional position variable (this is analogous to time-dependent density functional theory in quantum mechanics[23]).

3 Dynamical Density Functional Theory Formalism

The above motivate the derivation of a *dynamical density functional theory (DDFT)*, i.e. an equation of the form $\partial_t \rho(\mathbf{r}_1, t) = -\nabla_{\mathbf{r}_1} \cdot \mathbf{a}(\mathbf{r}_1, t, [\rho])$, where \mathbf{a} is a functional of ρ . The earliest and most basic DDFTs, as suggested by Evans[24] and derived by Marconi and Tarazona[15], neglect both inertia and HI. An improved version that still neglects inertia but includes two-body HI was recently given by Rex and Löwen[13]. Finally, Archer[14] derived a DDFT which includes inertia but neglects HI. All these DDFTs are special cases of our general formulation presented here, which includes both inertia and HI. Neglecting the HI terms in this new formulation trivially returns Archer's DDFT, whilst considering the high-friction limit recovers the configuration-space DDFTs[15, 13]; see later. This, along with the comparisons to the full stochastic simulations described below, serves as a validation of our generalized DDFT.

We denote the position and momentum of the j th particle by \mathbf{r}_j and \mathbf{p}_j and let $\mathbf{\Gamma}(\mathbf{r}) = \gamma[\mathbf{1} + \tilde{\mathbf{\Gamma}}(\mathbf{r})]$, where the HI tensor $\tilde{\mathbf{\Gamma}}$ is decomposed into 3×3 blocks $\tilde{\mathbf{\Gamma}}_{ij}$ [16]. Physically, $\tilde{\mathbf{\Gamma}}_{ij}$ describes how the momentum of particle j generates a force on particle i .

To obtain a reduced model for the Kramers equation, we consider its moments with respect to momentum and obtain an infinite hierarchy of equations. The challenge is now to find a suitable truncation of this hierarchy; this is analogous to deriving the Euler or Navier-Stokes equation from the Boltzmann equation[25]. We truncate the hierarchy at the second equation, giving a continuity equation

$$0 = \partial_t \rho(\mathbf{r}_1, t) + \nabla_{\mathbf{r}_1} \cdot (\rho(\mathbf{r}_1, t) \mathbf{v}(\mathbf{r}_1, t)) \quad (3)$$

and an equation for the time evolution of the current:

$$0 = \partial_t(\rho(\mathbf{r}_1, t)\mathbf{v}(\mathbf{r}_1, t)) + \gamma\rho(\mathbf{r}_1, t)\mathbf{v}(\mathbf{r}_1, t) + \frac{N}{m} \int d\mathbf{r}' \nabla_{\mathbf{r}_1} V(\mathbf{r}, t) \rho^{(N)}(\mathbf{r}, t) \quad (\text{V})$$

$$+ \frac{N\gamma}{m} \sum_{j=1}^N \int d\mathbf{p} d\mathbf{r}' \tilde{\Gamma}_{1j}(\mathbf{r}) \mathbf{p}_j f^{(N)}(\mathbf{r}, \mathbf{p}, t) \quad (\text{H})$$

$$+ \nabla_{\mathbf{r}_1} \cdot \int d\mathbf{p}_1 \frac{\mathbf{p}_1 \otimes \mathbf{p}_1}{m^2} f^{(1)}(\mathbf{r}_1, \mathbf{p}_1, t). \quad (\text{K})$$

Here $\rho^{(N)}(\mathbf{r}, t) = \int d\mathbf{p} f^{(N)}(\mathbf{r}, \mathbf{p}, t)$ is the N -body position distribution, $f^{(1)}(\mathbf{r}_1, \mathbf{p}_1, t) = N \int d\mathbf{p}' d\mathbf{r}' f^{(N)}(\mathbf{r}, \mathbf{p}', t)$ is the one-body phase-space distribution and $\rho(\mathbf{r}_1, t)\mathbf{v}(\mathbf{r}_1, t) = N/m \int d\mathbf{p} d\mathbf{r}' \mathbf{p}_1 f^{(N)}(\mathbf{r}, \mathbf{p}, t)$ is the current. To close the second equation as a functional of ρ and \mathbf{v} , it is necessary to deal with terms arising from the many-body part of the potential in (V), HI in (H), and ‘kinetic pressure’ effects in (K).

For (V), at equilibrium there exists an exact functional identity[24]

$$N \int d\mathbf{r}' \nabla_{\mathbf{r}_1} V(\mathbf{r}) \rho^{(N)}(\mathbf{r}) = \rho(\mathbf{r}_1, t) \nabla_{\mathbf{r}_1} \frac{\delta \mathcal{F}[\rho]}{\delta \rho} - k_B T \nabla_{\mathbf{r}_1} \rho(\mathbf{r}_1),$$

where \mathcal{F} is the Helmholtz free energy functional,

$$\mathcal{F}[\rho] = k_B T \int d\mathbf{r}_1 \rho(\mathbf{r}_1) [\ln(\Lambda^3 \rho(\mathbf{r}_1)) - 1] + \mathcal{F}_{\text{exc}}[\rho] + \int d\mathbf{r}_1 \rho(\mathbf{r}_1) V_1(\mathbf{r}_1),$$

where Λ is the Broglie wavelength, and plays no part in the following. In general, \mathcal{F}_{exc} (the excess over ideal gas term) is unknown but has been well-studied at equilibrium and good approximations exist, e.g. Rosenfeld’s fundamental measure theory[26, 12], which is accurate for hard spheres, and mean field theory[12], which becomes exact for soft interactions at high densities. Motivated by the success of such approximations in DFT, we assume that the same equilibrium identity also holds out of equilibrium. This has the further advantage of giving the correct equilibrium behaviour.

Since HI vanish at equilibrium there exists no analogous identity for (H). For ease of exposition, we assume that the HI are two-body: $\tilde{\Gamma}_{ij}(\mathbf{r}) = \delta_{ij} \sum_{\ell \neq i} \mathbf{Z}_1(\mathbf{r}_i, \mathbf{r}_\ell) + (1 - \delta_{ij}) \mathbf{Z}_2(\mathbf{r}_i, \mathbf{r}_j)$. We also assume that we may write the two-body reduced distribution[27] as $f^{(2)}(\mathbf{r}_1, \mathbf{r}_2, \mathbf{p}_1, \mathbf{p}_2, t) \approx f^{(1)}(\mathbf{r}_1, \mathbf{p}_1, t) f^{(1)}(\mathbf{r}_2, \mathbf{p}_2, t) g(\mathbf{r}_1, \mathbf{r}_2, [\rho])$ for a *known* functional g . Again, this has been well-studied at equilibrium[24]. To go beyond this two-body approach it is necessary to approximate higher-order reduced distributions as functionals of ρ .

As (K) is analogous to the kinetic pressure tensor[27], there is no reason to expect it to be a simple functional of ρ and \mathbf{v} . We are motivated by the local-equilibrium approximation widely used in statistical mechanics[27] and note that, for a general $f^{(1)}$, we have $f^{(1)}(\mathbf{r}_1, \mathbf{p}_1, t) = f_{\text{le}}^{(1)}(\mathbf{r}_1, \mathbf{p}_1, t) + f_{\text{neq}}^{(1)}(\mathbf{r}_1, \mathbf{p}_1, t)$, where $f_{\text{le}}^{(1)}$ is the local-equilibrium part, the momentum dependence of which is given by a local Maxwellian with mass $\rho(\mathbf{r}, t)$, mean $m\rho(\mathbf{r}, t)\mathbf{v}(\mathbf{r}, t)$ and variance $mk_B T \rho(\mathbf{r}, t)$. The corresponding mass, mean and variance of the non-equilibrium part $f_{\text{neq}}^{(1)}$ are all zero. The local-equilibrium part describes local quantities such as velocity and temperature, whilst the non-equilibrium part determines non-local quantities such as heat flux.

Combining these three approximations and denoting the material derivative $D_t = \partial_t + \mathbf{v}(\mathbf{r}_1, t) \cdot$

$\nabla_{\mathbf{r}_1}$ gives

$$\begin{aligned}
& D_t \mathbf{v}(\mathbf{r}_1, t) + \frac{1}{\rho(\mathbf{r}_1, t)} \nabla_{\mathbf{r}_1} \cdot \int d\mathbf{p}_1 \frac{\mathbf{p}_1 \otimes \mathbf{p}_1}{m^2} f_{\text{neq}}^{(1)}(\mathbf{r}_1, \mathbf{p}_1, t) \\
&= -\frac{1}{m} \nabla_{\mathbf{r}_1} \frac{\delta \mathcal{F}[\rho]}{\delta \rho} - \gamma \mathbf{v}(\mathbf{r}_1, t) \\
&\quad - \gamma \int d\mathbf{r}_2 \rho(\mathbf{r}_2, t) g(\mathbf{r}_1, \mathbf{r}_2, [\rho]) \mathbf{Z}_1(\mathbf{r}_1, \mathbf{r}_2) \mathbf{v}(\mathbf{r}_1, t) \\
&\quad - \gamma \int d\mathbf{r}_2 \rho(\mathbf{r}_2, t) g(\mathbf{r}_1, \mathbf{r}_2, [\rho]) \mathbf{Z}_2(\mathbf{r}_1, \mathbf{r}_2) \mathbf{v}(\mathbf{r}_2, t),
\end{aligned} \tag{4}$$

which, along with the continuity equation (3), and assuming that the term containing $f_{\text{neq}}^{(1)}$ may be neglected or approximated (e.g. via a Chapman-Enskog expansion) as a functional of ρ and \mathbf{v} , gives a DDFT. Neglecting this term can be rigorously motivated both close to local equilibrium, giving a generalised Navier-Stokes equation with non-local terms, and in the overdamped limit[16], recovering a new Smoluchowski equation with a novel diffusion tensor; see below. Note that (4) is non-local in both ρ and \mathbf{v} . These non-local terms, absent from previous DDFTs, model important correlations in the positions and velocities of different colloidal particles; we now discuss their physical interpretation. The term involving \mathbf{Z}_1 combines with $\gamma \mathbf{v}$ to give an effective, density-dependent friction coefficient, whilst that involving \mathbf{Z}_2 couples the velocities in a non-local fashion. Surprisingly, this coupling does not require explicit momentum correlations in the two-body distribution. These descriptions correspond to the physical interpretation of the associated friction tensor submatrices. Neglecting these terms and setting $f_{\text{neq}}^{(1)} = 0$ recovers a previous DDFT[14]. Furthermore, setting $\gamma = 0$ gives a DDFT for simple fluids, although in this case it is harder to justify neglecting the non-equilibrium term.

4 Verification and Numerical Experiments

We now describe three numerical tests of our proposed DDFT. In all cases we solve (3) and (4) for hard spheres of diameter 1, and choose $m = k_B T = 1$, which is equivalent to non-dimensionalizing the equations. We set $f_{\text{neq}}^{(1)} = 0$ and choose \mathcal{F} to be the hard-sphere FMT functional[26]. Further, we choose g to be the simplest possible pair correlation function $g(\mathbf{r}_1, \mathbf{r}_2, [\rho]) = 1$ for $|\mathbf{r}_1 - \mathbf{r}_2| > 1$ and zero otherwise, which describes the hard-sphere excluded volume. An extension would be to use the analytic correlation function based on the Percus-Yevick equation[28], but the above approximation suffices for the systems studied here.

In Figure 2 we compare the mean radial position and velocity of 50 particles, with friction coefficient $\gamma = 6$. The particles begin at equilibrium in a radially-symmetric external potential $V(r; 3)$ with minimum at radius 3. At time 0, the potential is instantaneously switched to $V(r; 0)$ with minimum at radius 0, which is then instantaneously switched back to $V(r; 3)$ at time 0.5. The choice of 50 particles is a compromise between requiring a large number of particles in order to overcome the differences between the canonical ensemble stochastic and grand canonical ensemble DDFT models, and computational complexity of the stochastic simulations. We show four pairs of computations, each containing the solutions of a DDFT (lines) and the corresponding underlying stochastic equation (squares). The first pair (blue) includes both inertia and HI and compares the solution of our generalized DDFT (3) and (4) to the Euler-Maruyama[20] solution of the stochastic equations (1). The second pair (red) are the same simulations, but when HI are neglected by setting $\mathbf{\Gamma} = \gamma \mathbf{1}$; this is the special case derived by Archer[14]. As far as we know, these are the first such numerical implementations of a phase space DDFT. In both cases, the agreement between the new DDFT and stochastic simulations is very good. The quantitative differences for the case including HI are due to an enforced difference in choice of friction tensor; see Materials and Methods. In addition, the effects of including HI are quite striking. In particular, HI appear to increase the effective friction of the system and damp the dynamics.

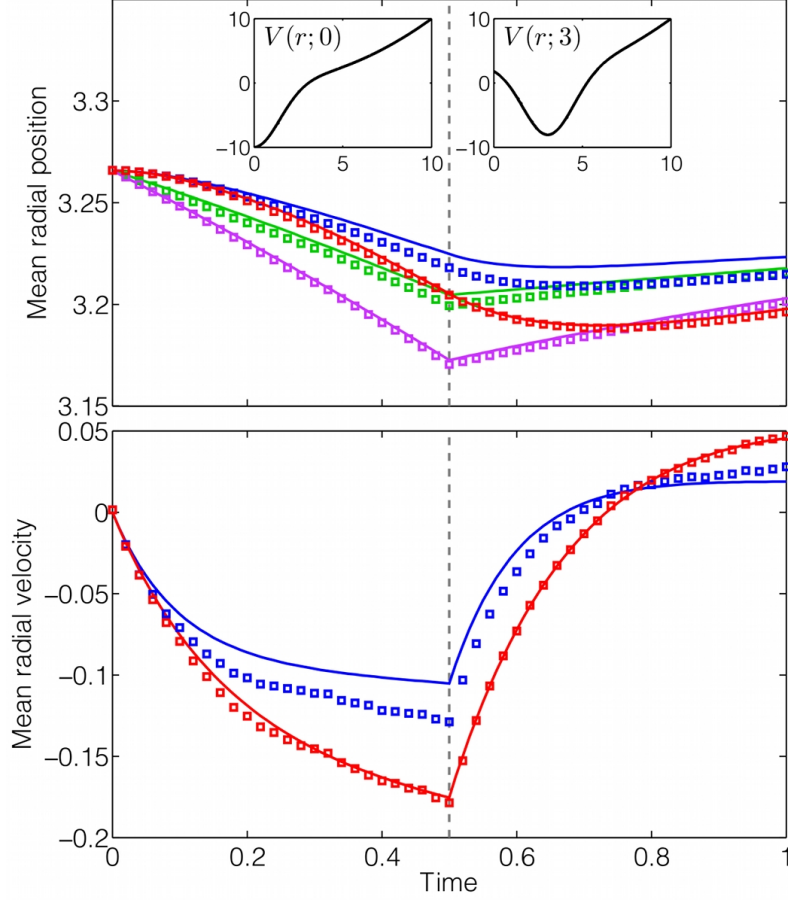


Figure 2: Mean radial positions and velocities given by (*lines*) DDFT and (*squares*) stochastic equations. Full phase space with (*blue*) and without (*red*) HI from DDFT (3) and (4) and stochastics (1). Overdamped limit DDFT[13] and stochastics[19] with (*green*) and without (*purple*) HI. The system contains 50 particles, has $\gamma = 6$, and starts at equilibrium in potential (6) with $r_0 = 3$, which is instantaneously switched to $r_0 = 0$ at time zero and then back to $r_0 = 3$ at time 0.5. See Materials and Methods for details.

The remaining two pairs of simulations are restricted to position space via the high-friction approximation, neglecting inertial effects. The DDFTs both with[13] (green) and without[15] (purple) HI are compared to the Ermak-McCammon[19] solution of the corresponding position-space stochastic equations. Whilst the agreement between DDFT and stochastic simulations is again very good, it is important to note that neglecting inertia leads to a qualitatively different behaviour of the system. In particular, it gives a kink in the mean position, whilst including inertia gives smooth curves with a delay before the mean velocity changes sign. Once again, HI are seen to significantly damp the dynamics.

In Figure 3 we show the evolution of the position distribution and velocity for the same system of particles, but we now only switch between potentials once, at time 0, and allow the particles to evolve towards equilibrium. Once again we compare the solutions of our generalized DDFT, both with (blue) and without (red) HI to the corresponding stochastic simulations. Again, the agreement between the DDFT and stochastic simulations is very good. The small differences in the position distribution near the origin (where the particle density is higher) are likely due to the choice of correlation function, which is less accurate at higher densities. Note in particular that the inclusion of HI dramatically slows the build-up of particles near the origin. Having verified

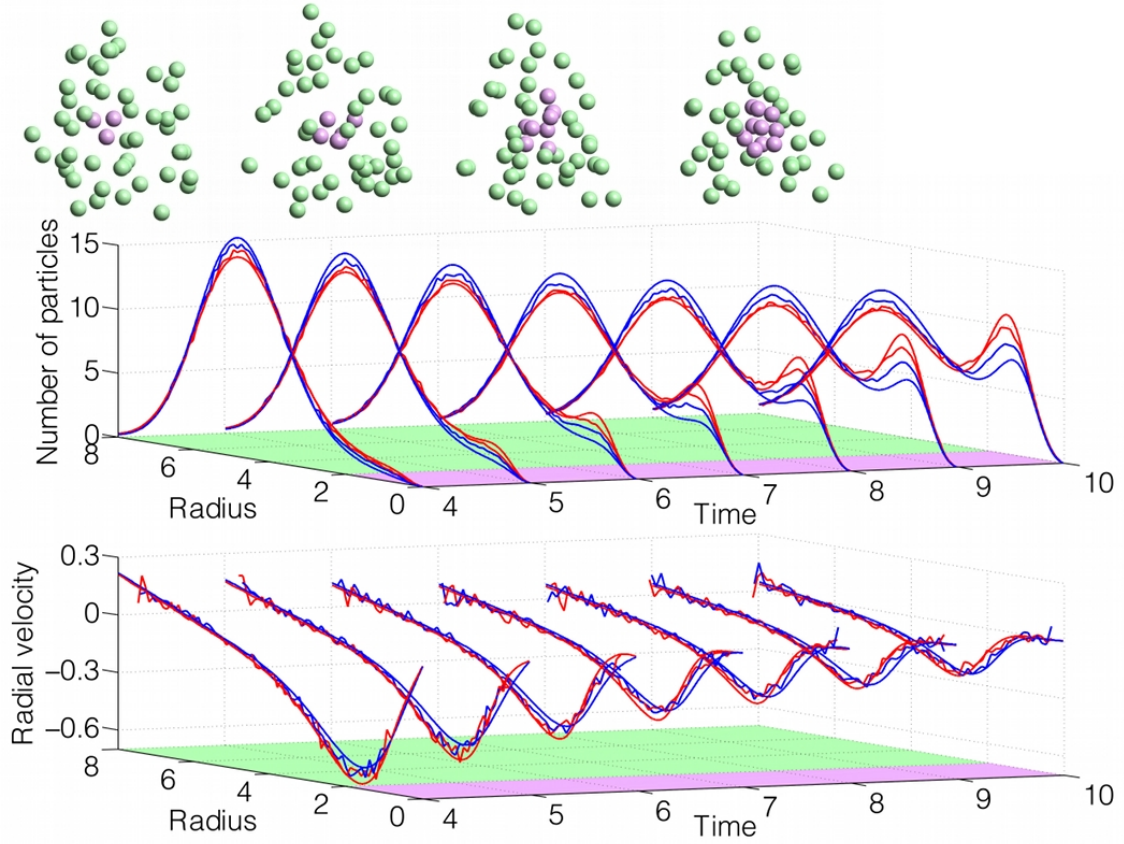


Figure 3: Radial particle distribution and velocity given by (*smooth curves*) solution of DDFT (3) and (4) versus (*noisy curves*) stochastic equations (1) with (*blue*) and without (*red*) HI. Also shown is one representative stochastic realization, at times 4, 6, 8 and 10, with particles coloured according to their radial position (*purple* denoting a radial position less than 2, *green* otherwise). The system contains 50 particles, with $\gamma = 6$, and starts at equilibrium in potential (6) with $r_0 = 5$, which is instantaneously switched to $r_0 = 0$ at time zero. See Materials and Methods for details and also Supplementary Movies 2 and 3.

our DDFT by comparison to stochastic simulations, Figure 4 depicts the evolution of the position distribution and velocity for the DDFT (3) and (4) with 500 particles, for which the stochastic equations are computationally very costly. In this case the effects of including HI are even more dramatic, giving qualitatively different behaviour of both the mass distribution and velocity for the DDFTs with and without HI. This size-dependence shows that HI must be carefully considered in any DDFT used to model macroscopic numbers of particles.

5 Connection with a Generalized Navier-Stokes Equation

For the remainder of this discussion we restrict our attention to a potential which is a sum of one- and two-body terms and discuss two limits of (4). Close to local equilibrium, we may expand $f^{(1)}$ and $f^{(2)}$ as Taylor series in $\nabla_{\mathbf{r}_1} \mathbf{v}$ [27], obtaining a generalized compressible, non-local Navier-Stokes-like integro-differential equation:

$$\rho D_t \mathbf{v} = \eta \nabla_{\mathbf{r}_1}^2 \mathbf{v} + (\zeta + \frac{1}{3} \eta) \nabla_{\mathbf{r}_1} (\nabla_{\mathbf{r}_1} \cdot \mathbf{v}) + \rho \mathcal{G}([\rho], [\mathbf{v}]),$$

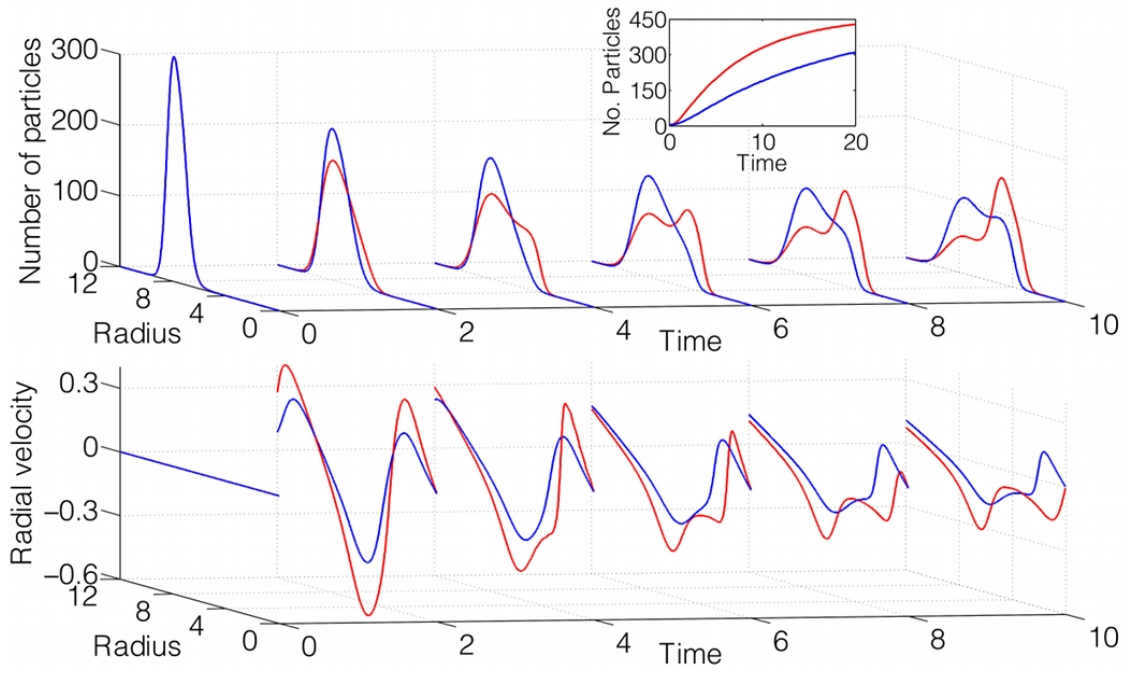


Figure 4: Radial particle distribution and velocity given by solution of DDFT (3) and (4) with (*blue*) and without (*red*) HI. The system contains 500 particles, with $\gamma = 10$, initially at equilibrium in potential (6) with $r_0 = 8$, which is instantaneously switched to $r_0 = 4$ at time zero. See Materials and Methods for details and also Supplementary Movies 4. Also shown are the number of particles with radii between 0 and 6.

where $\mathbf{v} = \mathbf{v}(\mathbf{r}_1, t)$, $\rho = \rho(\mathbf{r}_1, t)$ and $\mathcal{G}([\rho], [\mathbf{v}])$ is the right hand side of (4). The first three terms are standard in the compressible Navier-Stokes equation. However, the viscosities η and ζ are given by integrals involving the two-body potential and Taylor expansion coefficients of $f^{(1)}$ and $f^{(2)}$. Hence, the above equation is not amenable to a straightforward numerical solution. This restriction is not due to including HI; the same integrals occur when the statistical mechanics formulation of the pressure tensor is derived for a simple fluid[27]. The remaining terms (contained in \mathcal{G}) are a position-dependent pressure-like term which depends on the gradient of the chemical potential $\mu = \delta\mathcal{F}/\delta\rho$, and which is non-local in ρ , a friction term, and two additional non-local terms, the physical interpretation of which was discussed above.

6 The Overdamped Limit

As discussed above, most previous DDFTs have been formulated in the high-friction or overdamped regime. In such cases, it is assumed that the friction with the bath causes the momentum distribution of the colloidal particles to equilibrate on a much shorter timescale than their position distribution. Hence one is interested experimentally only in the position distribution whilst the momenta, and therefore inertia, may be neglected. In this regime, we have a non-dimensional parameter $\epsilon = \sqrt{k_B T / m \gamma}^{-1} L^{-1} \ll 1$, where L is a ‘typical’ length scale of the system. Denoting a Maxwellian momentum distribution by $M(\mathbf{p}_1) = \exp(-|\mathbf{p}_1|^2 / (2mk_B T)) / (2mk_B T \pi)^{3/2}$, we find rigorously[16] $f^{(1)}(\mathbf{r}_1, \mathbf{p}_1, t) = M(\mathbf{p}_1)(\rho(\mathbf{r}_1, t) + \epsilon \mathbf{a}(\mathbf{r}_1, t) \cdot \mathbf{p}_1 + \mathcal{O}(\epsilon^2))$ for some function \mathbf{a} ; in particular $\int d\mathbf{p}_1 (\mathbf{p}_1 \otimes \mathbf{p}_1) f^{(1)}(\mathbf{r}_1, \mathbf{p}_1, t) = \mathcal{O}(\epsilon^2)$. For ease of presentation, we assume $\mathbf{Z}_2 = 0$ (the case $\mathbf{Z}_2 \neq 0$ in the overdamped limit is rigorously analysed in reference [16]) and let $\rho^{(2)}(\mathbf{r}_1, \mathbf{r}_2, t) = \rho(\mathbf{r}_1, t)\rho(\mathbf{r}_2, t)g(\mathbf{r}_1, \mathbf{r}_2)$. Then the mass distribution ρ satisfies a Smoluchowski equation

$$\begin{aligned} \partial_t \rho(\mathbf{r}_1, t) = & \nabla_{\mathbf{r}_1} \cdot \left(\mathbf{D}(\mathbf{r}_1, [\rho]) \left[\frac{1}{k_B T} \nabla_{\mathbf{r}_1} V_1(\mathbf{r}_1, t) \rho(\mathbf{r}_1, t) \right. \right. \\ & \left. \left. + \nabla_{\mathbf{r}_1} \rho(\mathbf{r}_1, t) + \frac{1}{k_B T} \int d\mathbf{r}_2 \rho^{(2)}(\mathbf{r}_1, \mathbf{r}_2, t) \nabla_{\mathbf{r}_1} V_2(\mathbf{r}_1, \mathbf{r}_2) \right] \right), \end{aligned} \quad (5)$$

where we have a novel, density-dependent diffusion tensor:

$$\mathbf{D}(\mathbf{r}_1, [\rho]) = \frac{k_B T}{m \gamma} \left[\mathbf{1} + \int d\mathbf{r}_2 g(\mathbf{r}_1, \mathbf{r}_2) \rho(\mathbf{r}_2, t) \mathbf{Z}_1(\mathbf{r}_1, \mathbf{r}_2) \right]^{-1}.$$

Note that since (5) is non-linear in ρ , it is not the Fokker-Planck equation of a Langevin equation. Further, (5) can be transformed into a DDFT using standard arguments, but it differs from that derived by Rex and Löwen[13] under analogous assumptions. This is due to the non-commutativity of taking the overdamped limit and integrating over all but one particle.

In contrast to the standard definition, e.g. in reference [13], \mathbf{D} is a non-local functional of the density and thus is also implicitly time-dependent. Surprisingly, this arises even though the friction tensor is time-independent.

The resulting DDFT has the capacity to model significantly more complicated dynamics in a much wider range of systems. Previous phenomenological attempts at including a density-dependent diffusion coefficient in DDFTs do not correctly take into account the form of the diffusion tensor[29].

7 Conclusion

Through the inclusion of both inertia and HI, the new DDFT proposed here is general and can readily be applied to model a wide spectrum of real-world problems. Some representative applications in which we expect the new DDFT not only to provide accurate predictions but also help us elucidate the associated underlying phenomena include: (i) the rate, magnitude and pattern of aerosol and nanoparticle deposition in the respiratory system, where including inertia qualitatively changes predicted micro- and macroscale deposition, and HI with the walls affect flow

patterns; (ii) transport and coagulation of nanoparticles in pulsatile and oscillatory systems, such as oscillatory flow mixing, where both inertial and HI effects can quantitatively change the particle dynamics (as with the oscillatory system in Figure 2); and, (iii) cloud formation and aerosol production of fine powders, where particle inertia is responsible for preferential concentration and HI strongly influence clustering effects. Furthermore, there are many promising extensions to the modelling approach proposed here, e.g. to self-propelled particles, modelling bacteria; multiple particle species; anisotropic particles; and the inclusion of an external flow field, as would be required in modelling blood and drug-laden nanoparticle movement in blood. Similar modelling approaches should also be highly relevant in granular media, ion transport, and other multi-phase systems.

8 Methods

Potential We choose an external potential

$$V(r; r_0) = 0.1(1 - h)r^2 + 3h - 10 \exp[-(r - r_0)^2/4], \quad (6)$$

which consists of an asymptotically quadratic confining term, with h a smooth cutoff function $h(r) = [\text{erf}((r + r_0)/2) - \text{erf}((r - r_0)/2)]/2$, a constant term on the cutoff region, and an inverted Gaussian centred at r_0 .

Solution of stochastic equations The stochastic equations (1) are solved using a standard Euler-Maruyama scheme with 10^5 time steps. Each simulation is averaged over 5000 runs, the initial conditions being chosen via slice sampling the (unnormalized) equilibrium N -body distribution $f^{(N)}(\mathbf{r}, \mathbf{p}) = \exp(-V(\mathbf{r})/k_B T) \exp(-|\mathbf{p}|^2/(2mk_B T))$. The hard sphere potential is approximated via a slightly softened, differentiable one[13].

Solution of DDFT equations We assume that $\rho(\mathbf{r}_1, t)$ and $\mathbf{v}(\mathbf{r}_1, t)$ are functions of only $|\mathbf{r}_1|$, producing a 1D problem. We use spectral methods[30], appropriately extended to integral operators, and a fifth order implicit Runge-Kutta method with step size control[31]. The initial condition is obtained by solving the equilibrium DFT equation[24].

Friction and diffusion tensors Since $\mathbf{\Gamma}$ in (1) must be positive-definite, we use the inverse of the Rotne-Prager approximation with hydrodynamic diameter $\sigma_H = 0.5$ [13]. This choice of σ_H justifies both neglecting lubrication forces and using a two-body expansion. For the DDFT (3) and (4) we use the 11-term two-body expansion given by Jeffrey and Onishi[21]. Whilst not strictly equivalent, the two descriptions are similar when the particles are well-separated in terms of the hydrodynamic diameter. In the overdamped limit, the Rotne-Prager approximation to the diffusion tensor is used for both stochastic and DDFT calculations.

Acknowledgments We thank Petr Yatsyshin for stimulating discussions regarding free-energy functionals. We are grateful to the European Research Council via Advanced Grant No. 247031, the Rotary Clubs Darmstadt, Darmstadt-Bergstraße and Darmstadt-Kranichstein, the European Framework 7 via Grant No. 214919 (Multiflow) and the Engineering and Physical Sciences Research Council of the UK via grant No. EP/H034587/ for support of this research.

References

- [1] R. Brown. A brief account of microscopical observations made on the particles contained in the pollen of plants. *Phil. Mag.*, 4:161–173, 1828.
- [2] A. Einstein. The presumed movement of suspended particles in static fluids. *Ann. Phys. Lpz.*, 17:549–560, 1905.

- [3] P. Langevin. Sur la théorie du mouvement brownien. *C. R. Acad. Sci. (Paris)*, 146:530–533, 1908.
- [4] M. Von Smoluchowski. Über Brownische Molekularbewegung unter Einwirkung äusserer Kräfte und deren Zusammenhang mit der verallgemeinerten Diffusionsgleichung. *Ann. Phys.*, 48:1103–1112, 1915.
- [5] J. Perrin. Mouvement Brownien et réalité moléculaire. *Ann. Chim. Phys.*, 18:1–114, 1909.
- [6] T. Franosch, M. Grimm, M. Belushkin, F.M. Mor, G. Foffi, L. Forró, and S. Jeney. Resonances arising from hydrodynamic memory in Brownian motion. *Nature*, 478(7367):85–88, 2011.
- [7] R. Huang, I. Chavez, K.M. Taute, B. Lukić, S. Jeney, M. G. Raizen, and E. L. Florin. Direct observation of the full transition from ballistic to diffusive Brownian motion in a liquid. *Nature Physics*, 7(7):576–580, 2011.
- [8] E. Matijević, editor. *Medical Applications of Colloids*. Springer, New York, 2008.
- [9] D. F. Evans and H. Wennerström. *The Colloidal Domain: Where Physics, Chemistry, and Biology Meet*. Wiley, New York, 1999.
- [10] H.A. Stone and S. Kim. Microfluidics: Basic issues, applications and challenges. *AIChE J.*, 47:1250–1254, 2001.
- [11] F. Caruso. *Colloids and Colloid Assemblies: Synthesis, Modification, Organization and Utilization of Colloid Particles*. Wiley, Weinheim, 2004.
- [12] J. F. Lutsko. Recent developments in classical density functional theory. *Adv. Chem. Phys.*, 144:1, 2010.
- [13] M. Rex and H. Löwen. Dynamical density functional theory for colloidal dispersions including hydrodynamic interactions. *Eur. Phys. J. E*, 28:139–146, 2009.
- [14] A. J. Archer. Dynamical density functional theory for molecular and colloidal fluids: A microscopic approach to fluid mechanics. *J. Chem. Phys.*, 130(1):014509, 2009.
- [15] U. M. B. Marconi and P. Tarazona. Dynamic density functional theory of fluids. *J. Chem. Phys.*, 110(16):8032–8044, 1999.
- [16] B. D. Goddard, G. A. Pavliotis, and S. Kalliadasis. The overdamped limit of dynamical density functional theory: Rigorous results. *arXiv:1108.3185v1*, 2011.
- [17] J. K. G. Dhont. *An Introduction to Dynamics of Colloids*. Elsevier, 1996.
- [18] J. T. Padding and A. A. Louis. Hydrodynamic interactions and Brownian forces in colloidal suspensions: Coarse-graining over time and length scales. *Phys. Rev. E*, 74:031402, 2006.
- [19] D. L. Ermak and J. A. McCammon. Brownian dynamics with hydrodynamic interactions. *J. Chem. Phys.*, 69(4):1351–1360, 1978.
- [20] P. E. Kloeden and E. Platen. *Numerical Solution of Stochastic Differential Equations*. Springer-Verlag, Berlin, 1992.
- [21] D. J. Jeffrey and Y. Onishi. Calculation of the resistance and mobility functions for two unequal rigid spheres in low-Reynolds-number flow. *J. Fluid Mech.*, 139(1):261–290, 1984.
- [22] G. K.-L. Chan and R. Finken. Time-dependent density functional theory of classical fluids. *Phys. Rev. Lett.*, 94:183001, 2005.

- [23] M. A. L. Marques, C. A. Ullrich, F. Nogueira, A. Rubio, K. Burke, and E. K. U. Gross, editors. *Time-Dependent Density Functional Theory*, volume 706 of *Lect. Notes Phys.* Springer, Berlin, 2006.
- [24] R. Evans. The nature of the liquid-vapour interface and other topics in the statistical mechanics of non-uniform, classical fluids. *Adv. Phys.*, 28(2):143–200, 1979.
- [25] P. Résibois and M. De Leener. *Classical Kinetic Theory of Fluids*. Wiley, 1977.
- [26] Y. Rosenfeld. Free-energy model for the inhomogeneous hard-sphere fluid mixture and density-functional theory of freezing. *Phys. Rev. Lett.*, 63(9):980–983, 1989.
- [27] H. J. Kreuzer. *Nonequilibrium Thermodynamics and Its Statistical Foundations*. Oxford University Press, New York, 1981.
- [28] A. Trokhymchuk, I. Nezbeda, J. Jirsák, and D. Henderson. Hard-sphere radial distribution function again. *J. Chem. Phys.*, 123:024501, 2005.
- [29] M. Rauscher. DDFT for Brownian particles and hydrodynamics. *J. Phys. Condens. Matter*, 22:364109, 2010.
- [30] J. P. Boyd. *Chebyshev and Fourier Spectral Methods*. Dover, UK, 2001.
- [31] E. Hairer and G. Wanner. *Solving Ordinary Differential Equations II. Stiff and Differential-Algebraic Problems*, volume 14 of *Springer Series in Computational Mathematics*. Springer-Verlag, Berlin, 2006.